PCP
PLANT & CELL PHYSIOLOGY

Changes in Membrane Lipid Composition and Function Accompanying Chilling Injury in Bell Peppers

Ximan Kong[1,3], Baodong Wei[1,3], Zhu Gao[1], Ying Zhou[2], Fei Shi[1], Xin Zhou[1], Qian Zhou[1] and Shujuan Ji[1,*]

[1]Post-harvest Biology and Storage of Fruits and Vegetables laboratory, Department of Food Science, Shenyang Agricultural University, 110866, China
[2]College of Life Science, Sun Yat-sen University, 510275, China
[3]These authors contributed equally to this work.
*Corresponding author: E-mail, jsjsyau@yeah.net or jsjsyau@sina.com; Fax +86-24-88498337.
(Received August 2, 2017; Accepted November 6, 2017)

Bell peppers are vulnerable to low temperature (<7°C) and subject to chilling injury (CI). To elucidate the relationship between cell membrane lipid composition and CI, a membrane lipidomic approach was taken. In addition, we performed microstructural analysis and low-field nuclear magnetic resonance to better understand CI. We also monitored primary physiological metabolism parameters to explain lipidomics. Our study indicated that cellular structure damage was more serious at 4°C, mostly represented by damage to the plasmalemma and plastid degradation. Membrane lipidomic data analysis reveals monogalactosyldiacylglycerol, phosphatidylcholine, phosphatidylethanolamine and phosphatidic acid as crucial biomarkers during CI. Furthermore, the significant increase in proline, electrolyte leakage and phospholipase D in chilled fruits also proved that membrane lipid metabolism is involved in the response to low temperature stress. To our knowledge, this study is the first attempt to describe the CI mechanisms in bell peppers based on membrane lipidomics.

Keywords: Bell peppers • Chilling injury • Membrane lipidomics • Cellular structure.

Abbreviations: CI, chilling injury; DGDG, digalactosyldiacylglycerol; LC-MS, liquid chromatography–mass spectrometry; LF-NMR, low-field nuclear magnetic resonance; LPC, lyso-phosphatidylcholine; LPE, lyso-phosphatidylethanolamine; LPG, lyso-phosphatidylglycerol; MDA, malondialdehyde; MGDG, monogalactosyldiacylglycerol; MRI, magnetic resonance imaging; PA, phosphatidic acid; PC, phosphatidylcholine; PE, phosphatidylethanolamine; PG, phosphatidylglycerol, PI, phosphatidylinositol; PLD, phospholipase D; PS, phosphatidylserine; qRT–PCR, quantitative reverse transcription–PCR; ROS, reactive oxygen species; SEM, scanning electron microscopy; SFR2, sensitive to freezing 2; TEM, transmission electron microscopy.

Introduction

Bell peppers (*Capsicum annuum* L.), an important agricultural product, have high economic value and nutrient content. It is known for its high vitamin C content and human health benefits (Rwm et al. 2004, Mateos et al. 2013). To guarantee freshness and extend post-harvest quality, bell peppers need to be stored at a low temperature. However, peppers are quite susceptible to chilling injury (CI) at low temperature, especially below 7°C (González-Aguilar et al. 2000, Wang et al. 2016). The main CI symptoms which appear in peppers are surface pitting, calyxes, seed darkening, and shrinkage due to moisture loss (Hardenburg et al. 1990).

From a physiological viewpoint, improper chilling will cause metabolic disturbance of the cytomembrane, resulting in the excessive accumulation of reactive oxygen species (ROS), which finally leads to injury in plants (Wise 1995, Zeng et al. 2015). The cell membrane is important not only for its function of perception and barrier but also for supporting internal physiological metabolism. When it comes to extreme environments, such as cold, plants have to adapt membrane composition in order to maintain organelle function (Ernst et al. 2016). Recent studies have shown that the cytomembrane becomes less fluid when temperature decreases. To maintain normal fluidity of membranes, the degree of unsaturation in the membrane lipids increases (De 2014, Holthuis and Menon 2014). In addition, chilling could induce cellular oxidation and result in oxidative stress due to excess ROS (Malacrida et al. 2006). Consequently, the major components of the cell membrane are destroyed and eventually cause oxidative damage (Nejadsadeghi et al. 2015).

Lipidomic approaches have been utilized for cold acclimation for over a decade (Welti et al. 2002). In recent years, enhanced plant lipidomic methods based on liquid chromatography–mass spectrometry (LC-MS) have provided us with more comprehensive insights about the responses of membrane lipid composition and functions to chilling (Pablo et al. 2015). Under cold stress, besides the increase in the degree of fatty acid unsaturation, the main constituent component of chloroplast-specific lipid is also susceptible, such as a decrease in monogalactosyldiacylglycerol (MGDG) (Moellering et al. 201, Szymanski et al. 2014). Additionally, a notable increase in phosphatidic acid (PA), lyso-phosphatidylcholine (LPC) and lyso-phosphatidylethanolamine (LPE) is another response to low temperature. Usually, this process proceeded along with the involvement of phospholipase D (PLD). A number of studies indicate that PLD plays an important role in the regulation of membrane lipid composition during cold signaling (Hong et al. 2016). However, the related studies have focused on model plants, such as Arabidopsis, whereas the cold stress response

Plant Cell Physiol. 59(1): 167–178 (2018) doi:10.1093/pcp/pcx171, Advance Access publication on 9 November 2017, available online at www.pcp.oxfordjournals.org

mechanism in non-model plants such as bell peppers during post-harvest storage remains unclear. To date, the relevant reports about bell pepper storage have been mainly concerned with changes in post-harvest quality and the transcriptome (Lee and Choi, 2013, Li et al. 2015, Wang et al. 2016). In this work, a membrane lipidomic study in bell peppers accompanying CI has been carried out based on automated electrospray ionization–tandem mass spectrometry technology.

In addition, microscopic investigation has been used to visualize the effects on the cellular structure in bell pepper tissues caused by CI. Ultrastructural analysis has shown that the subcellular organelle changes during storage. This analysis, combined with physiological and metabolic information, makes it easier to explain the metabonomics of membrane lipids and understand the mechanisms resulting in membrane damage from CI.

At present, CI symptoms in fresh agricultural products during storage and transportation have become a serious problem, whereas the injury mechanism based on membrane lipidomics is not fully clear. There are few reports about eukaryotic cells, especially plant cells. In a previous study (Liu et al. 2015), we characterized the changes in structure and fatty acids during low temperature storage. This study aimed to elucidate the CI mechanism in bell peppers by analyzing the composition of membrane lipids at different temperatures. We also monitored CI symptoms in peppers from the macrocosm to the microcosm and, finally, we measured physiological indices to verify the CI response.

Results

Modification of membrane lipids composition

We identified approximately 100 molecular species of polar lipids with different carbon numbers in pepper samples using a lipidomic method employing an automated electrospray ionization–tandem mass spectrometer. Among the 100 lipid molecular species, there were two categories of galactolipids [MGDG and digalactosyldiacylglycerol (DGDG)], six categories of phospholipids [PA, phosphatidylcholine (PC), phosphatidylethanolamine (PE), phosphatidylglycerol (PG), phosphatidylinositol (PI) and phosphatidylserine (PS)] and three categories of lysophosphatides [LPC, LPE and lyso-phosphatidylglycerol (LPG)]. The total lipid content was 174.9, 120.5 and 57.6 nmol mg^{-1} DW in fresh samples, and those stored at 10 and 4°C, respectively. Compared with the fresh group, the level of total membrane lipids declined regardless of storage temperature, with a notable decline at 4°C (**Fig. 1A**). The contents of MGDG, the main galactolipid, decreased by approximately 30% and 70% in 10 and 4°C, samples, respectively, in contrast to the fresh group. Additionally, the degradation of PC was reduced from 20.8 to 4.2 nmol mg^{-1} DW (10°C) and 3.03 nmol mg^{-1} DW (4°C) (**Fig. 1B**). In contrast, the level of DGDG increased in the samples at 10 and 4°C. The DGDG:MGDG ratio increased from 0.09 to 0.26 (10°C) and 0.42 (4°C), respectively. The remaining membrane lipids slightly decreased.

We observed a trend in increased DGDG and decreased PC, PE and PG. The relative change in composition in membrane lipids is shown in **Fig. 1C, D**. The percentage of PA and total lysophosphatides at 4°C was higher than that in the fresh and 10°C groups. The major contributors to MGDG degradation were 36:6 and 34:2 molecular species, and to a lesser extent 36:1 (**Fig. 1F**). Accordingly, these molecular species, as well as 36:3, increased in DGDG. As the main component of phospholipid, the content of 34:2 and 36:4 PC and PE was reduced dramatically. For instance, the percentage of 36:4 PC at 4°C decreased 32.9%, twice as much as at 10°C. For the content of PG, 34:3 molecular species clearly changed, dropping 20.7% and 32.6% at 10 and 4°C, respectively. Additionally, the percentage of 36:4 PA went up substantially among the main constituents of 34:2, 36:4 and 36:5 PA. Furthermore, it showed a slight increase in 36:6 PA.

Cellular structural changes

Structural changes in anatomy. We observed quality changes in bell pepper fruits during the whole storage period. Bell peppers are composed of calyx, seeds and pericarp (exocarp, mesocarp and endocarp). In general, the exocarp has a layered cell structure, with cells arranged tightly without intercellular spaces. The same is true for endocarp cells, whereas an obvious distinction between them is that exocarp cells have a hypertrophic cell wall. The volume of mesocarp cells is relatively large and the intercellular space is distinct because of the loose multilayer arrangement.

Fresh pepper fruits (newly harvested) had a clear line between the exocarp and mesocarp (**Fig. 2D**). Additionally, the arrangement of collenchyma and parenchyma cells was ordered. Compared with the fresh pepper fruits (**Fig. 2A**), there was no evident change in the control group except for a slightly brown stain on the carpopodium (**Fig. 2B**). However, both the pericarp lines and cellular arrangement gradually became blurred after anatomical structure observation (**Fig. 2E**). The CI group fruits showed significant injury such as surface pitting and severe brown staining caused by cold stress (**Fig. 2C**). Also, unclear collenchyma and parenchyma cell outlines could be observed in the 4°C samples (**Fig. 2F**). Furthermore, the pepper texture weakened, exocarp was depressed and flesh was folded.

Structural changes in cellular morphology. Structure information of the cellular morphology of plant tissue is often detected using scanning electron microscopy (SEM). We used SEM to study the morphological structure of fresh peppers and peppers stored at 10 and 4°C. For fresh samples, the cell size was homogeneous (**Fig. 3A**), and the whole cellular profile was clearly visible. The rounded cells had an intact cell wall and interior materials. However, the cell size of pepper tissue stored at 10°C showed heterogeneity and slight corrugations. The cellular morphology was irregular and the intercellular space increased (**Fig. 3B**). In bell peppers stored at 4°C, we observed a non-integrated cellular structure and a badly damaged histological structure. The degree of cellular shrinkage was obvious, and a few visible folds existed in cell walls and membranes.

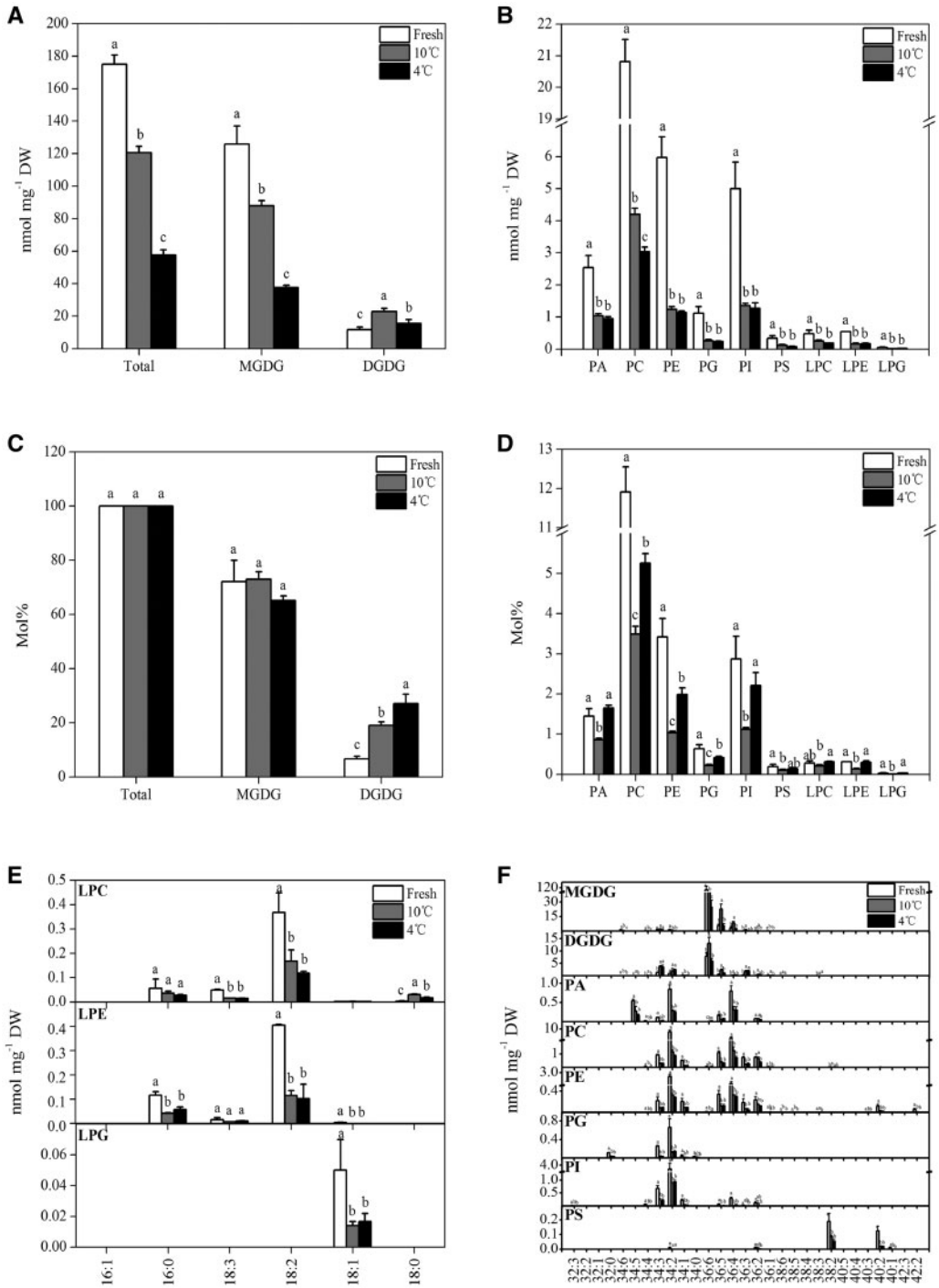

Fig. 1 Changes of lipid composition and proportion in fresh, 10°C 20th day and 4°C 20th day samples during storage. (A) Total lipid and glycolipid composition changes during storage; (B) phospholipid composition changes during storage; (C) total lipid and glycolipid proportion changes during storage; (D) phospholipid proportion changes during storage; (E and F) glycolipid and phospholipid molecular species composition changes during storage. Values in the same column with different letters are significantly different ($P < 0.05$). Values represent averages and the SD of three biological replicates ($n = 3$). DGDG, digalactosyldiacylglycerol; LPC, lyso-phosphatidylcholine; LPE, lyso-phosphatidylethanolamine; LPG lyso-phosphatidylglycerol; MGDG, monogalactosyldiacylglycerol; PA, phosphatidic acid; PC, phosphatidylcholine; PE, phosphatidylethanolamine; PG, phosphatidylglycerol, PI, phosphatidylinositol; PS, phosphatidylserine.

Ultrastructural changes in bell peppers. Subcellular structure was observed to elucidate the changes during CI. The collenchyma cells of fresh peppers possessed abundant organelles (**Fig. 4A1**) in comparison with the 10 and 4°C samples. The chloroplasts attached tightly to the cell walls due to the pressure of the vacuole. The intercellular space in the parenchyma cells was full of material (**Fig. 4A2**) compared with the other groups. Furthermore, numerous lamellar thylakoids and a few

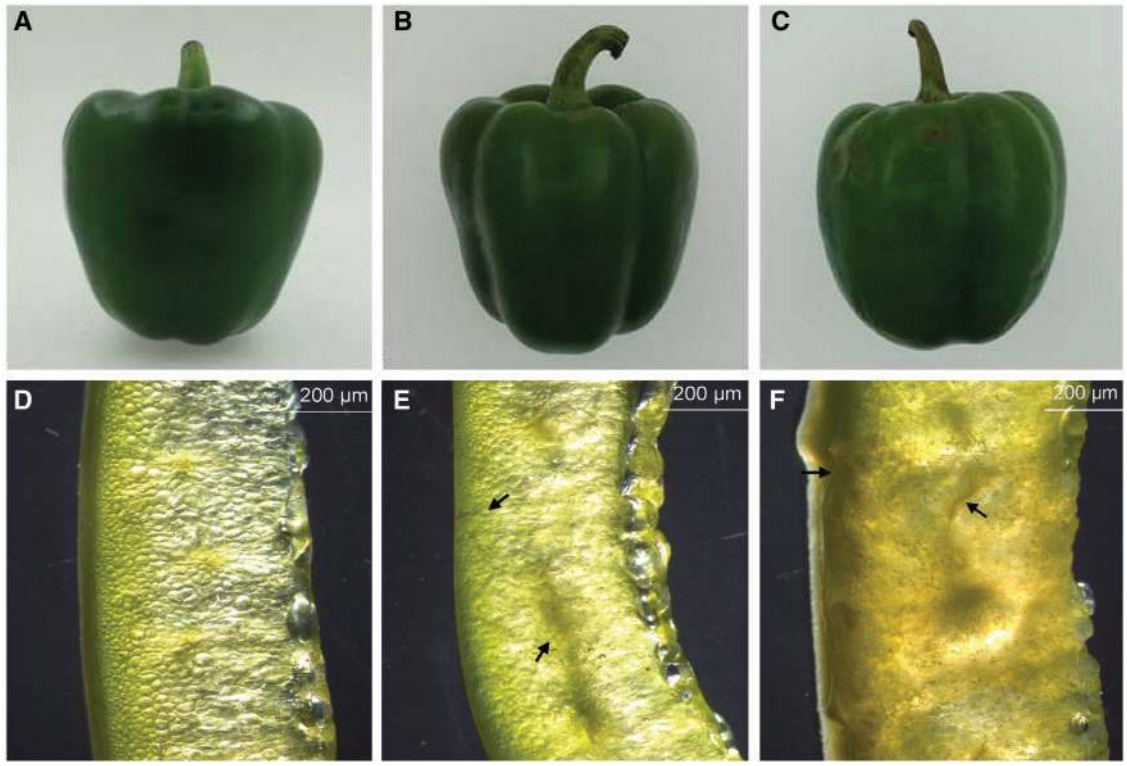

Fig. 2 Changes of apparent and anatomical structure in fresh (A, D), 10°C 20th day (B, E) and 4°C 20th day (C, F) samples during storage. The arrows in (E) point to a collenchymatous cell and parenchymal cell, respectively. The arrows in (F) point to a depression and fold, respectively.

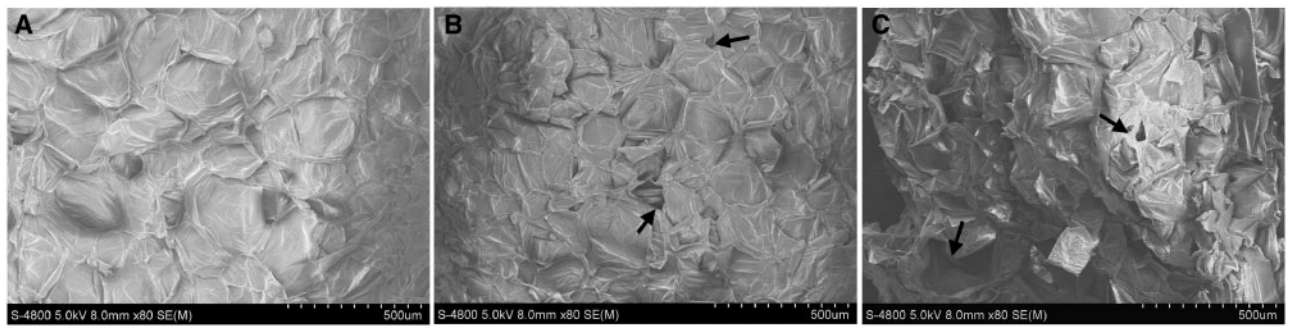

Fig. 3 Changes of cell morphological structure in fresh (A), 10°C 20th day (B) and 4°C 20th day (C) samples. The arrows in (B) point to the intercellular space. The arrows in (C) point to the fold and split, respectively.

globular starch grains existed in the shuttle-like chloroplasts (**Fig. 4A4**), in addition to a few plastoglobuli. However, the morphology of cellular organelles changed greatly during storage, especially in the CI group (4°C). For the control group, the boundary between cell walls and the cytomembrane was clear (**Fig. 4B3**), and the chloroplasts began to swell and appear spindle like (**Fig. 4B4**). The number of starch grains decreased, whereas that of plastoglobuli started to increase. This phenomenon was most notable in samples storage at 4°C. The cell walls were contorted (**Fig. 4C1**) and plasmolysis appeared (**Fig. 4C3**). The chloroplasts were almost round, and the internal structure became indistinct, mainly in the thylakoids. The starch grains were barely visible, and the content of the plastoglobuli was much higher than in the fresh and 10°C samples (**Fig. 4C4**).

Water distribution and NMR image

Low-field nuclear magnetic resonance (LF-NMR) has been widely used in evaluating the water state of different food materials, such as soybean, orange and tofu (Lin et al. 2016). To determine the inner connection between water proton dynamics and subcellular structure, we monitored the T_{2i} relaxation time and corresponding water population M_{2i} (**Table 1**) in bell peppers. Generally, the process of CI begins with the calyx, and then extends to the fruit surface, seeds and finally to whole fruit rot. Therefore, the top of the bell pepper (containing the calyx) was cut for moisture measurement and LF-NMR imaging. As shown in **Fig. 5**, both fresh and 4°C samples had four proton fractions: T_{21}, T_{22}, T_{23} and T_{24}, whereas there were three proton fractions in the 10°C samples: T_{21}, T_{22} and T_{23}.

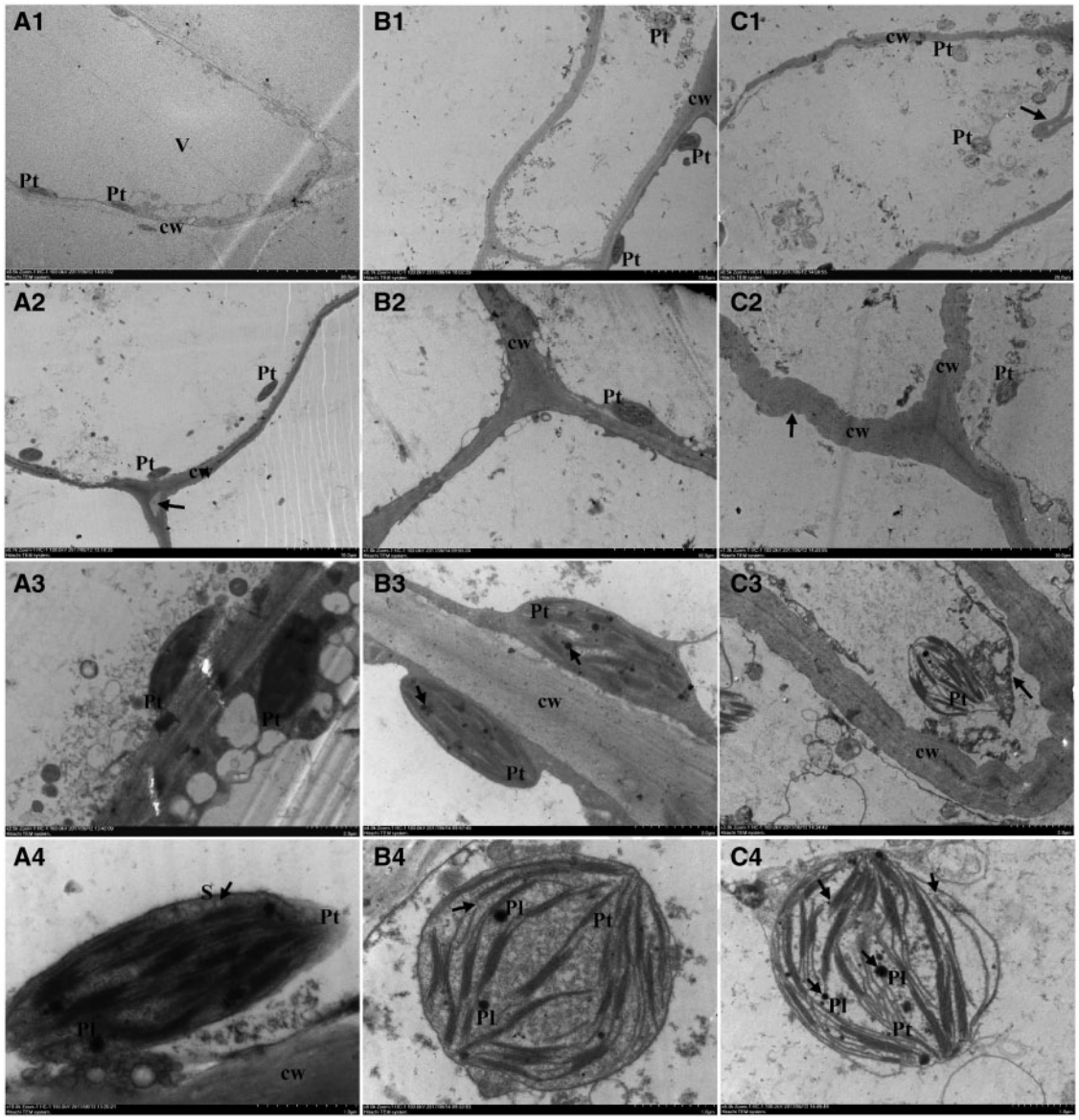

Fig. 4 Ultrastructure changes in fresh (A1, A2, A3, A4), 10°C 20th day (B1, B2, B3, B4), and 4°C 20th day (C1, C2, C3, C4) samples. CW, cell wall; Pl, plastoglobuli; Pt, plastid; S, starch grain; V, vacuole. The arrows in (A2) and (A4) indicate the intercellular space and a starch grain. The arrows in (B3) and (B4) represent plastoglobuli and a fractured thylakoid. The arrows in (C1) and (C2) indicate the cell wall fold. The arrows in (C3) indicate plasmolysis. The arrows in (C4) indicate plastoglobuli and a fractured thylakoid.

Table 1 The corresponding relative amount (M_{2i}) of relaxation times (T_{2i}) in bell peppers at different storage temperatures

Treatment condition	M_{21} (%)	M_{22} (%)	M_{23} (%)	M_{24} (%)
Fresh	1.48 ± 0.00^{b}	1.90 ± 0.01^{c}	19.15 ± 0.04^{c}	79.14 ± 0.10
10°C	1.67 ± 0.01^{b}	4.38 ± 0.01^{b}	94.32 ± 0.02^{a}	–
4°C	2.07 ± 0.00^{a}	9.73 ± 0.03^{a}	42.53 ± 0.12^{b}	45.68 ± 0.15**

Values are means ± SD.
Values in the same column with different letters are significantly different ($P < 0.05$).
**$P < 0.01$.

This showed that the number and proportion of relaxation components were changed due to different storage temperatures. According to previous studies on plant tissues (Snaar and Van As 1992, Hills and Remigereau 1997), the slowest relaxation component, T_{24}, represented the presence of free water molecules in the vacuole. In our experiment, M_{24} accounted for >80% of the water proton population in fresh samples, whereas it was <50% in CI samples (4°C). The second relaxation

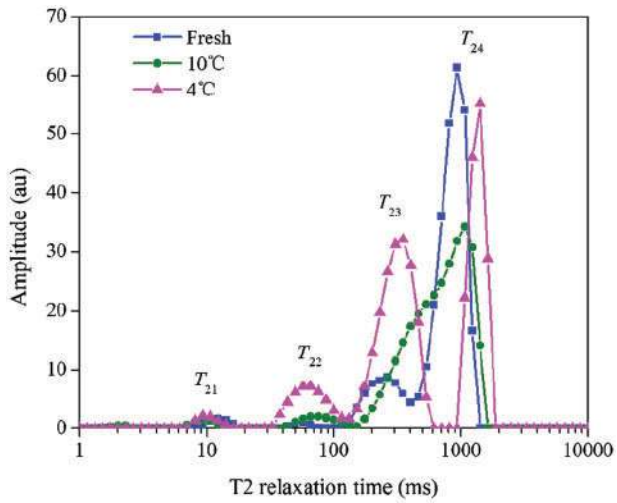

Fig. 5 Low-field nuclear magnetic resonance (LF-NMR) T_2 relaxation time curves in fresh, 10°C 20th day and 4°C 20th day samples. T_{21}, T_{22} and T_{23} represented the transverse relaxation time of the bound water molecules which is combined with organic matter tightly like proteins. T_{24} refers to the transverse relaxation time of free water molecules.

component, $T_{23,}$ was considered as cytoplasmic water and there was a significant change in the water proton population among samples. For fresh samples, the proton population (M_{23}) was approximately 20%, whereas it climbed to >40% in 4°C samples. It is noteworthy that the relaxation components T_{24} and T_{23} in 10°C samples merged into one peak. We assume that this kind of water status was a transitional period and both of the components will redistribute in the later stage. In other words, the free water was transforming into bound water whereas this transformation processes had not ended yet. The third relaxation component, T_{22}, was identified as extracellular water and the proportion (M_{22}) was 1.90, 4.38 and 9.73% in fresh, 10 and 4°C samples, respectively. The fastest relaxation component, T_{21}, was regarded as bound water distributed in the cell wall. Approximately 2% of the proton population (M_{21}) was present in all the samples. Compared with the T_2 relaxation component in the fresh samples, the water status in CI group samples has changed a lot. The free water relative content decreased and the bound water relative content increased. It was likely that a part of water protons has been transferred from the vacuole to the cytoplasm.

In contrast to LF-NMR measurement of T_2 relaxation time, the moisture distribution and proton fluidity inside the tissues can be directly detected using magnetic resonance imaging (MRI). The fresh peppers had high moisture content, therefore the images presented as bright with a red color in most areas (**Fig. 6A, D**). Furthermore, the linkage between the calyx and sarcocarp was rather tight. For the samples stored at 10°C, the red area decreased and the blue area increased, and there was separation from the calyx to sarcocarp. This indicated that the moisture content was reduced (**Fig. 6B, E**). However, the moisture density of the 4°C samples was significantly decreased in both the sarcocarp and calyx, and the linkage was vague.

Proline content, MDA content and electrolyte leakage

Proline is one of the protein components in plants. It not only adjusts cytoplasm osmosis, but also plays an important role in tolerance to abiotic stresses such as cold, salt and drought. Therefore, the changes in proline content during storage were analyzed. The results are shown in **Fig. 7A**. Compared with the control group, the proline accumulation at 4°C increased apparently during the whole storage period. The proline content of the 4°C group reached 65.9 μg g^{-1} FW, which was more than three times higher than the 10°C group on the 20th day.

Malondialdehyde (MDA) is the end-product of lipid oxidation, and therefore it is considered to be one of the main indicators of oxidative damage (Xu et al. 2009). The results of MDA content determination at both storage temperatures showed an increasing trend over the whole storage time. Furthermore, on the 20th day, the MDA content at 4 and 10°C was 1.18 and 1.04 nmol g^{-1} FW, respectively. Notably, CI symptoms became visible at this time. This result revealed that MDA content was much higher when bell peppers suffered from chilling. It also explained the rapid deterioration of plastid in the 4°C samples.

Changes in membrane permeability during storage were evaluated by determining the electrolyte leakage. As shown in **Fig. 7B**, electrolyte leakage of each treatment increased with the extension of storage time. During storage at 4°C, the increased amplitude was more notable. Moreover, the electrolyte leakage at 4 and 10°C during the later stage of storage (the 20th day) was 38.45% and 30.08%, respectively, and the percentage of the CI group was higher compared with the control.

PLD activity analysis and gene expression

PLD plays an important role in cell regulation, metabolism and plasma membrane integrity. It is also the initial enzyme in lipid catabolism (Hong et al. 2016). Therefore, PLD activity in bell pepper stored at different temperatures was measured. As reported in **Fig. 7D**, an increase in PLD activity at both 4 and 10°C was observed. At the beginning of storage, PLD activity in the CI group increased significantly, especially on the fifth day, probably a stress response due to rapid change in environmental temperature after harvest. PLD activity in peppers exposed to 4°C was higher than at 10°C during storage.

We previously designed and amplified a *PLD* gene (GenBank MF996861) which had a high genetic relationship with *Capsicum annuum PLDα4*. To detect the gene expression of *PLDα4*, quantitative reverse transcription–PCR (RT–qPCR) was performed. As shown in **Fig. 7E**, there was a visible difference between the CI group and control. The *PLDα4* expression level of the CI group was the highest on the fifth day, which was more than three times that in the control, and then decreased by degrees. As for the control, the relative expression quantity of *PLDα4* increased with storage time, and then began to decrease after 15 d.

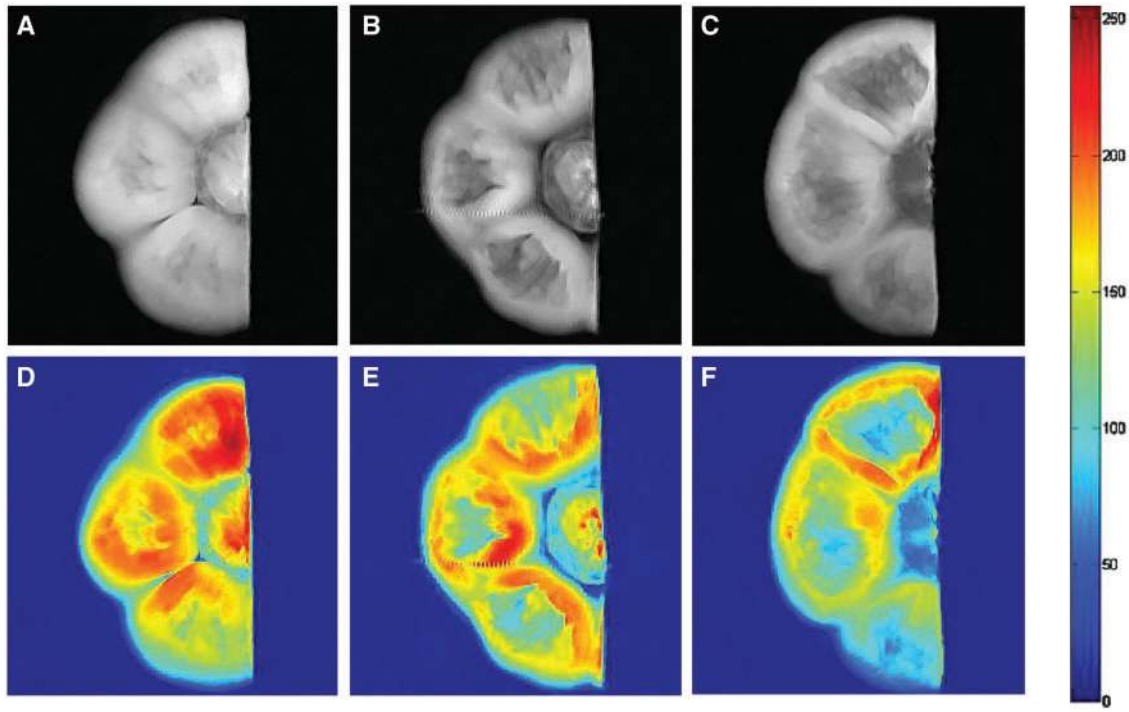

Fig. 6 Nuclear magnetic resonance (NMR) images in fresh (A, D), 10°C 20th day (B, E) and 4°C 20th day (C, F) samples. The images were color-coded based on their grayscale value. Red corresponded to the 'bright part' and blue to the 'dark part'.

Discussion

Cold stress greatly altered membrane lipid composition and proportion

Membrane lipids play an important role in supporting regular physiological metabolism by maintaining cellular fluidity and permeability. To our knowledge, cells can adjust their membrane lipid composition when suffering from environmental stress. Thereby, a lipidomic approach was carried out to analyze the lipid redistribution in bell peppers at different storage temperatures. Our results showed that the level of total membrane lipids decreased with decreased storage temperature. These changes are mainly reflected in MGDG and PC. It was recognized that conical MGDG molecules easily converted to cylindrical DGDG to maintain the stability of thylakoid membranes during cold and osmotic stress (Pablo et al. 2015, Gasulla et al. 2016). In addition, self-disintegration was another cause for the decrease of MGDG. Sensitive to freezing 2 (SFR2), a protein necessary during this process, has been proved to mediate the remodeling of the chloroplast envelope membranes by transferring galactolipid residues from the abundant monogalactolipid to different galactolipid acceptors, forming oligogalactolipids and diacylglycerol (Moellering et al. 2010). PC and PE were predominant phospholipids in fresh samples, whereas they both decreased at 4°C perhaps due to the cold-induced activation of the PLD pathway. *PLDα1* and *PLDδ* have been positively demonstrated to hydrolyze structural phospholipids into PA in responses to cold stress. (Welti et al. 2002, Rajashekar et al. 2006). Moreover, the excess PA could further generate hydroperoxides and free radicals with a series of enzymes, and finally lead to plasma membrane damage (Li et al. 2009). The higher percentage of PA at 4°C in our experiments also provides evidence of membrane lipid remodeling due to cold stress. Likewise, the high percentage content of lysophosphatides at 4°C, especially of LPC and LPE, provided proof for the degradation of PC and PE, too. Lysophospholipids as signaling lipid are derived from the hydrolysis of the membrane lipids and then are released into the extracellular space where they can be recognized by extracellular receptors and initiate signaling pathways (Hou et al. 2016).

Besides the response to cold stress, the membrane lipid changes were more likely to be induced by dehydration stress. MRI analysis indicated that the water content was reduced in bell pepper tissues during storage. One of the first symptoms in dehydration injury is the decline in membrane lipid contents (Gigon et al. 2004). Numerous studies have recorded that the increase in the DGDG to MGDG ratio is the most conspicuous response to dehydration stress (Torres-Franklin et al. 2007); the change trend of the DGDG:MGDG ratio in our studies was no exception. Furthermore, the dark color of pepper cells in anatomical structure at 4°C may be relevant to the decrease in MGDG. Thus we can deduce that the SFR2 pathway was activated to stabilize the bilayer in both cold and dehydration stress. Another recognized response to dehydration stress is the increase in the activity of catabolic enzymes (Gigon et al. 2004). As a major enzyme in phospholipase catabolism, PLD was greatly accumulated during storage at 4°C in our experiment.

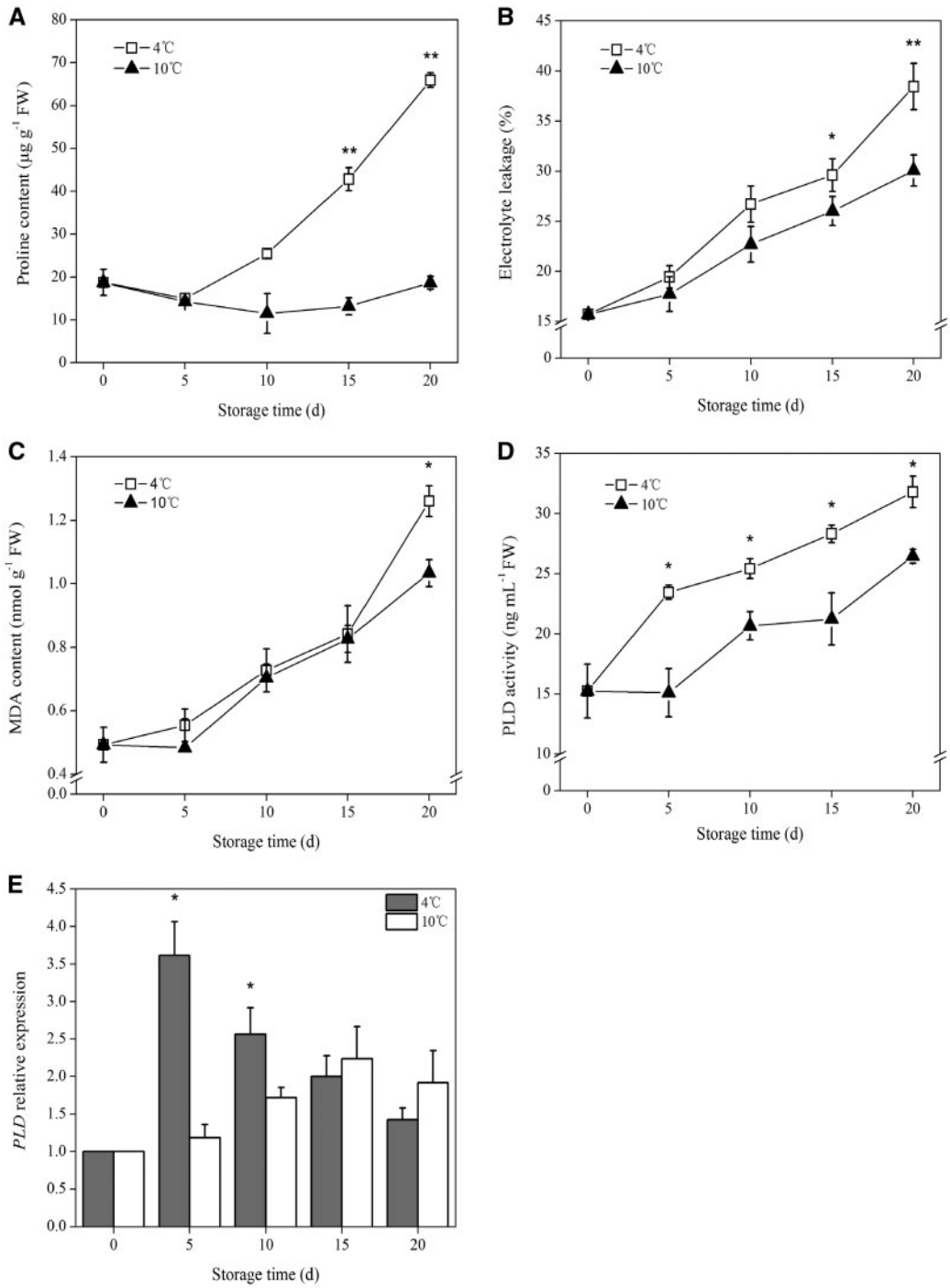

Fig. 7 Physiological changes in proline content (A), electrolyte leakage (B), MDA content (C), PLD activity (D) and *PLD* gene expression (E) of bell peppers at 10 and 4°C during storage. Each value is the mean of three replicates of 10 fruits and error bars represent the SD of the means ($n = 3$). $^{*}P < 0.05$; $^{**}P < 0.01$.

Cellular structures are seriously damaged during the CI process

In this study, histological structure changes in bell peppers during storage were observed in order to understand CI on a celluar level. The cellular arrangement of bell peppers is complex; there are approximately 20 layers of cells in the flesh. Mesocarp cells account for most of them, including collenchyma and parenchyma. Collenchyma is the primary place for chloroplast development, so this part presents a green color. However, the color of these cells was dim, especially at 4°C. One of the main causes for this may be the disintegration of Chl caused by ROS accumulation in the thylakoid membrane. Additionally, cellular profiles were vague at both temperatures, especially for parenchyma. It is possible that the parenchyma had a thinner cell wall and was more easily damaged compared with collenchyma. Consequently, cellular electrolytes flowed

outward, leading to vague profiles. For the CI group, there was obvious pitting in exocarp and folding in parenchyma. It is likely that the intracellular macromolecular structures were badly damaged and finally resulted in tissue collapse. These similar microstructural changes have been previously described in other breeds such as chili pepper fruits (Liu 2013). Surface pitting in fruits is a major performance indicator during CI. It is confirmed that plasmalemma is the main site of CI, and plasmalemma will lose its ability to act as a barrier to resist cold (Yamada et al. 2002). Thus, intracellular electrolytes migrate from outwards. Cellular adhesion is reduced and intercellular space increased. This injury mechanism is common in plant cells which are sensitive to cold. Our results also indicated that the morphological structure of pepper cells, including cell walls and membranes, was seriously damaged during cold stress (4°C).

The preceding lipidomic results in our work showed the decline in MGDG, PC and PE during storage. Accordingly, transmission electron microscopy (TEM) analysis offered a better understanding of these changes. The breakdown in chloroplast structure at 4°C confirmed the sharp reduction in MGDG, because MGDG was a major chloroplast membrane lipid. The detachment and folding of plasmalemma were consistent with the decrease in PC and PE. In addition, another performance indicator in the plasmalemma was the changes in thickness. The cytomembrane at 4°C became a little thicker compared with fresh samples. It was a response to low temperature of membrane lipid. Some of the recent studies on membrane lipid have shown that plasmalemma become less fluid when temperatures decrease, and, as compensation, the level of unsaturated fatty acids increases (De 2014, Holthuis and Menon 2014). It was the unsaturated double bonds that made the membranes thicker (Sinensky 1974, Saita et al. 2016). Thus, cell membrane damage is more easily seen at low temperatures.

In addition, the water distribution in CI group pepper tissues also indicated that the permeability of the tonoplast was enhanced and the tonoplast structure was damaged. The increase in extracellular and cell wall water in the 4°C samples indicated plasma membrane damage and cell wall degradation. Coincidentally, this water distribution in our pepper fruits was also present in other fruits such as apples and sweet corn (Marigheto et al. 2008, Shao and Li 2013). These moisture changes helped us comprehend the membrane lipid remodeling at a deeper level, similar to TEM results. The above changes in cellular structure revealed that low temperature had a more severe influence on pepper fruits.

Regulation of physiological metabolism in response to cold stress

Proline has many crucial functions for higher plant responses to abiotic stress, such as osmotic adjustment, protecting cellular structures, as an antioxidant and as a signaling substance. Many studies have confirmed that the accumulation of proline content increased markedly when plants were subjected to environmental stress (Zeng et al. 2015, Lei et al. 2016). This physiological phenomenon is mainly reflected in the increased proline synthesis, decreased proline degradation and proline transportation. In general, the glutamate pathway is the main process for proline synthesis, and Δ1-pyrroline-5-carboxylate synthetase (P5CS) is a key enzyme for proline synthesis. Many studies have shown that the enzymatic activity of P5CS and the corresponding *P5CS* gene expression increased when plants were in an extreme environment (Sharma and Verslues 2011, Bagdi and Shaw 2013). As a result, the free proline content increased to resist adverse stress. Our results also showed that there was a significant difference in proline content between the control group and CI group.

When plants are subjected to abiotic stress, such as cold, the ROS inside plant cells constantly accumulate and cause lipid oxidation. Finally, physiological metabolism of cells was disordered, leading to membrane damage. MDA is the oxidation end-product in this pathway. Wang et al. (2012, 2016) determined that the MDA content increased in bell peppers stored at 3°C, as in our study. In addition, similar results were also shown in other plants such as wheat and bamboo shoots (Nejadsadeghi et al. 2015, Zeng et al. 2015). As with MDA, electrolyte leakage is also an important sign of membrane damage. In the current study, severe changes at 4°C confirmed cytomembrane damage. The function of the cell membrane becomes unbalanced when plants are exposed to chilling for a long time, damaging the cell membrane and decreasing membrane permeability (Meng et al. 2012).

It is generally acknowledged that low temperature is good for the storage of fruits and vegetables. However, it may also cause chilling damage. When plants are subjected to cold stress, the concentration of cytosolic Ca^{2+} increases in response to low temperature, and then the *PLD* gene is activated and expression leads to higher PLD activity (Laxalt et al. 2001, Testerink and Munnik 2011, Aghdam et al. 2016). Accordingly, the membrane phospholipid is degraded and PA accumulation increases, leading to membrane damage (Tiwari and Paliyath 2011). PA could be generated through two pathways: the PLD pathways producing PA and choline/ethanolamine via the hydrolysis of PC and PE, and the PLC/diacylglycerol kinase (DGK) pathway (Munnik and Laxalt 2013). Our work consistently showed a significant decrease in PC and increases in PA and PLD activity of the CI group. This phenomenon indicated that the PLD pathway was activated in cold stress. Similar activity also appeared in other plants such as Arabidopsis plants and anthurium cut flowers (Aghdam et al. 2016, Muzi et al. 2016). However, the transcription level of *PLDα4* showed some discrepancies compared with PLD activity. The reason for this difference might be because *PLDα4* is one of the *PLD* gene family members, and the transcription level of different gene families is discrepant under abiotic stress. Research has shown that *PLDα1* and *PLDδ* are induced markedly by drought and salt stresses (Katagiri et al. 2001, Bargmann et al. 2004); furthermore, the transcription level of *PLDδ* is higher when plants meet with chilling (Li et al. 2004). Despite the above, it is certain that the *PLDα4* gene made a great contribution to PLD activity in the CI group in the early days of storage. Higher PLD activity later in storage may be due to other *PLD* genes. To our knowledge, there have

been hardly any reports about *PLDα4*, while most research is focused on *PLDα1* and *PLDα3*.

Conclusion

This work explored deterioration in bell pepper quality in response to low temperature based on metabolism of membrane lipidomics. We systematically monitored the changes in cellular structure and primary physiological parameters. Our results indicated that low temperature (4°C) caused serious membrane damage. An omics analysis revealed that MGDG, PC, PE and PA could be regarded as biomarkers not only in cold stress but also in dehydration stress. We also confirmed that the PLD pathway was activated earlier and played a dominant role during cold stress. In addition, the SFR2 pathway may also mediate the remodeling of the chloroplast envelope membranes under cold stress. Overall, our research offered a new insight into how CI in post-harvest fruits and vegetables results from low temperature. However, the cold signal conduction mechanism and expression of the genes responsive to cold induced by a transcription activator are still not clear. In the future, we will make an in-depth exploration of the molecular mechanism of the involvement of the signaling lipids in response to cold stress.

Materials and Methods

Plant material and sample treatment

Bell peppers (*Capsicum annuum* L., cv 'Sanxing') were picked from an ecological farm in Anshan, Liaoning, China, and transported immediately to the laboratory. Pepper fruit selection was based on size uniformity, no mechanical injury, carpopodium intactness and similar maturity. The fruits were packaged in PVC film bags (0.03 mm) after pre-cooling, then randomly divided into three groups, each with three biological replicates. The harvested samples were defined as the first group, the second group was the samples stored at 10°C (control) and the third group was the samples stored at 4°C (chilled samples). Each treatment included 100 pepper fruits. The relative humidity was kept at 80% for all samples. Membrane lipid composition, microstructure and moisture distribution were analyzed on the day of harvest and the 20th day. The other physiological parameters were measured every 5 d. All experiments were performed when the samples recovered to room temperature.

Extraction of nembrane lipids

Membrane lipids were extracted according to Welti et al. (2002). Pepper tissues that had been cut from the same position were quickly transferred into 3 ml of pre-heated dimethylcarbinol [containing 0.01% butylated hydroxytoluene (BHT)] and water baths for 15 min at 75°C. Then 1.5 ml of chloroform and 0.6 ml of ultrapure water were added into the tubes, 150 g min^{-1} for 1 h. The extracted solution was then transferred into glass tubes. The lipid extraction was repeated with 4 ml of $CHCl_3$/MeOH (2 : 1, v/v) containing 0.01% BHT, 150 g min^{-1} for 30 min and transferred again. We repeated the above steps until the samples became discolored. We combined the extracted solution and added 1 ml of 1 M KCl, then centrifuged it at 500 × *g* for 5 min and discarded the water phase. Next, 2 ml of ultrapure water was added to the extract, centrifuged at 500 × *g* for 5 min and the water phase was discarded. The solvent from the membrane lipid extract was evaporated under a stream of N_2 and stored at −80°C. The post-extraction samples were dried overnight at 105°C and subsequently weighed.

Membrane lipids were measured according to Xiao et al. (2010) and via automated electrospray ionization–tandem mass spectrometry.

Histomorphological observation

Anatomical structure investigation of bell pepper. Longitudinal sections of bell peppers from different storage temperatures (harvest, 4°C and 10°C) were observed using a stereo microscope (LEICA, M165 C). Images were acquired with a digital CCD camera. Samples were put on a plate and images were taken at the location where the laser light was applied.

Cellular morphological observation. Peeled samples (3 mm × 5 mm) were quickly fixed overnight in 2.5% glutaraldehyde (v/v) at 4°C until tissues sank. Then the stationary phase liquid was removed and cleaned with 0.1 M phosphate buffer (pH 7.2) three times, each step for 15 min. After that, the samples were dehydrated using an ethanol series of increasing concentrations (50, 70, 80, 90 and 95%) for 15 min successively. Next, the samples were dehydrated twice in a 100% ethanol solution for 15 min. Finally, anhydrous ethanol was displaced with isoamyl acetate for 15 min and dried. For observation of samples, conductive silicone was applied to adhere the samples to the stage and then the samples were coated with gold for 30 s using a sputter coater (Hitachi E-1010). All the samples were observed with an S-4800 (Hitachi) scanning electron microscope at 5.0 kV electron beam.

Ultrastructural observation. Pre-fixation (1 mm × 1 mm × 3 mm) was the same as for SEM. Post-fixation was conducted in 1% osmium tetroxide for 2 h and then samples were washed with phosphate buffer three times. After that, dehydration proceeded with an increasing series of ethanol (50% and 70%) and acetone (80% and 90%) for 15 min each. Then the samples were dehydrated three times in 100% acetone for 30 min. The samples were soaked in a mix of propylene oxide and SPI-812 embedding medium. Finally, samples were immersed overnight in embedding medium. Ultrathin sections (50 nm1) were cut using a Leica EM UC7 ultramicrotome and collected on copper grids. Then the ultrathin sections were stained with uranyl acetate followed by lead citrate, and detected using a Hitachi HT7700 transmission electron microsope.

LF-NMR measurements

LF-NMR was performed using a 23.3 MHz NMR Analyzer MesoMR23-060H-I (Niumag Co., Ltd.) to measure water distribution, and MRI was carried out as described in Han et al. (2008). Approximately 10 g FW from the top of the pepper samples were cut and placed on the LF-NMR probe. The transverse relaxation time (T_2) was measured using the Carr–Purcell-Meiboom–Gill (CPMG) sequence. The CPMG parameters were set as spectral width (SW), 100 kHz; pulse at 90° (P1), 18 μs; pulse at 180° (P2), 37 μs; waiting time (TW), 8,000 ms; radio frequency delay time (RFD), 0.08 ms; analog gain (RG1), 20 db; digital gain (DRG1), 3; and echo time (TE), 0.6 ms. Data from 10,000 echoes were acquired with four scan repetitions. The relaxation measurements were conducted at 32°C. MultiExp Inv Analysis software (Niumag Co., Ltd.) was used for data analysis by performing multi-exponential fitting on T_2 relaxation data. The relaxation time (T_{2i}) and its corresponding water population (signal area ratio) (M_{2i}) were recorded.

For the MRI detection of samples, spin echo sequence was carried out. Repetition time (TR) and echo time (TE) were 2,000 μs and 19 μs, respectively. The read size was set to 256, phase size was 192 and RG was 10 db. Slice width was 20 mm and slice gap was 2 mm. Later, a series of gray water proton density LF-NMR images of samples were obtained. These images were color-coded based on their grayscale value. Red corresponded to the 'bright part' and blue to the 'dark part'.

Determination of MDA and electrolyte leakage

The determination of MDA content was performed according to Meng et al. (2012). Pepper samples (1.0 g FW) were homogenized in 5 ml of 10% (w/v) trichloroacetic acid (TCA) and centrifuged at 12,000 × *g* for 30 min. The supernatant (2 ml) was added into 2 ml of 0.67% (w/v) thiobarbituric acid (TBA), then the mixture was kept in boiling water for 15 min. Next, the mixture was instantly cooled down in an ice bath and centrifuged at 10,000 × *g* for 10 min. The absorbance of the supernatant was measured at wavelengths of 450, 532 and 600 nm, and the MDA content was calculated using the following formula

$$MDA(nmol\,g^{-1}FW) = [6.45 \times (A_{532} - A_{600}) - 0.56 \times A_{450}] \times V_t/(V_S \times m)$$

where V_t and V_s are the total volume of the extract solution and the volume of the extract solution contained in the reaction mixture solution, respectively; m is the mass of the sample.

Electrolyte leakage determination was performed according to Mao et al. (2007). Discs of pepper tissues (4 mm in thickness) were separated by a cork borer with a 9 mm diameter. Then these discs were rinsed three times with deionized water and dried with filter paper. Fifteen discs of samples were put into a test tube with 20 ml of deionized water for 3 h at 25°C. After that, electric conductivity was measured with a conductivity meter (DDS-307). Then these tubes were placed in a boiling water bath for 30 min and cooled to room temperature until the conductivity was measured again. Electrolyte leakage was expressed as a percentage of the initial electrolyte leakage to reflect membrane permeability.

Proline content measurement

Proline content was detected according to Zhao et al. (2009) with some modification. Pepper fruits (2.0 g FW) were mixed with 5 ml of 3% (w/v) sulfosalicylic acid, then the mixture was transferred into test tubes. The tubes were kept in boiling water for 10 min and centrifuged at 10,000 × *g* for 20 min. A 2 ml aliquot of the supernatant was added into a mixture of glacial acetic acid (2 ml) and ninhydrin (3 ml), and the mixture was heated in boiling water for 30 min. After cooling, 4 ml of toluene was added into the tubes and they were shaken for 30 s. The absorbance of the proline–toluene phase (upper layer) was measured at 520 nm using a UV 5100 spectrophotometer (METASH). Proline content was calculated according to the proline standard curve and expressed as $\mu g\,g^{-1}$ FW.

PLD activity and RT–qPCR analysis

Bell pepper fruits (5 g FW) were homogenized in 5 ml pre-cooled phosphate-buffered saline (PBS) containing 0.1 M $Na_2HPO_4{\cdot}12H_2O$ and 0.1 M $NaH_2PO_4{\cdot}2H_2O$; this step was carried out on ice. After centrifuging at 8,300 r.p.m. for 20 min at 4°C, the supernatant was used for PLD activity assay. The measurement was performed according to the Plant Phospholipase D ELISA Kit Instruction. A standard curve for PLD was made from the A_{450} of the standard substance, and sample concentration was calculated using the standard curve.

Total RNA was extracted from pepper tissues using an OminiPlant RNA Kit (CWBIO), according to the manufacturer's instructions. After the integrity and concentration of RNA were determined, 0.09 μg of RNA was used for cDNA synthesized according to the HiFiScript cDNA Synthesis Kit (CWBIO). The *PLD* primers were designed using Primer 5.0 (forward primer 5′-ACAAAGG AGGGCCAAGAG-3′ and reverse primer 5′-ATGGGAATGAGCAAAGACG-3′). The RT–qPCRs were performed in a total volume of 20 μl containing 10 μl of 2 × UltraSYBR Mixture, 2 μl of cDNA template, 0.4 μl of primers (0.2 $\mu mol\,l^{-1}$) and 7.2 μl of ddH_2O. The PCR amplification profile was 95°C for 10 min, followed by 40 cycles of 95°C for 15 s, and 60°C for 1 min and subjected to melting curve analysis. Blank control and replicates were carried out for each treatment. The Ct values were transformed into relative quantitative data according to RT–qPCR. The mRNA levels were normalized to the *β-actin* transcriptional level (forward primer 5′-ACCTCATGCCATTCTTCG-3′ and reverse primer 5′-GACAATTTCCCGTTCAGC-3′), and the harvest (0 d) was regarded as the control to calculate $2^{-\Delta\Delta Ct}$.

Statistical analysis

All statistical analyses were performed with SPSS version 20.0 (SPSS Inc.). Data were analyzed using a one-way analysis of variance (ANOVA). Mean separations were performed using least significant difference (LSD). Differences at $P < 0.05$ were considered to be significant. Each experiment was repeated in triplicate.

Funding

This work was supported by the National Key R&D Program of China (2016YFD0400103).

Acknowledgments

We thank the College of Life Science (Dalian Minzu University) for SEM experiment observation. We thank Shanghai Niumag Corporation for their technical support with LF-NMR measurement.

Disclosures

The authors have no conflicts of interest to declare.

References

Aghdam, M.S., Naderi, R., Jannatizadeh, A., Sarcheshmeh, M.A.A. and Babalar, M. (2016) Enhancement of postharvest chilling tolerance of anthurium cut flowers by γ-aminobutyric acid (GABA) treatments. *Sci. Hortic.* 198: 52–60.

Bagdi, D.L. and Shaw, B.P. (2013) Analysis of proline metabolic enzymes in *Oryza sativa* under NaCl stress. *J. Environ. Biol.* 34: 677–681.

Bargmann, B.O., Laxalt, A.M., Ter, R.B., Van, S.B., Merquiol, E., Testerink, C., et al. (2009) Multiple PLDs required for high salinity and water deficit tolerance in plants. *Plant Cell Physiol.* 50: 78–89.

De, M.D. (2014) Temperature sensing by membranes. *Annu. Rev. Microbiol.* 68: 101–116.

Gasulla, F., Barreno, E., Parages, M.L., Cámara, J., Jiménez, C., Dörmann, P., et al. (2016) The role of phospholipase D and MAPK signaling cascades in the adaption of lichen microalgae to desiccation: changes in membrane lipids and phosphoproteome. *Plant Cell Physiol.* 57: 1908–1920.

Gigon, A., Matos, A.R., Laffray, D., Zuily-Fodil, Y. and Pham-Thi, A.T. (2004) Effect of drought stress on lipid metabolism in the leaves of *Arabidopsis thaliana* (ecotype Columbia). *Ann. Bot.* 94: 345–351.

González-Aguilar, G.A., Gayosso, L., Cruz, R., Fortiz, J., Báez, R. and Wang, C.Y. (2000) Polyamines induced by hot water treatments reduce chilling injury and decay in pepper fruit. *Postharvest Biol. Technol.* 18:L 19–26.

Han, M., Zhang, Y., Fei, Y., Xu, X. and Zhou, G. (2008) Effect of microbial transglutaminase on NMR relaxometry and microstructure of pork myofibrillar protein gel. *Eur. Food Res. Technol.* 228: 665–670.

Hardenburg, R.E., Watada, A.E. and Yang, C.Y. (1990) The Commercial Storage of Fruits, Vegetables, and Florist and Nursery Stocks. Agriculture Handbook, 66. Edited by Gross, K.C., Wang, C.Y. and Saltveit, M. USDA, Washington, DC.

Hills, B.P. and Remigereau, B. (1997) NMR studies of changes in subcellular water compartmentation in parenchyma apple tissue during drying and freezing. *Int. J. Food Sci. Technol.* 32: 51–61.

Holthuis, J.C.M. and Menon, A.K. (2014) Lipid landscapes and pipelines in membrane homeostasis. *Nature* 510: 48–57.

Hong, Y., Jian, Z., Liang, G., Kim, S.C., Deng, X., Wang, G., et al. (2016) Plant phospholipases D and C and their diverse functions in stress responses. *Prog. Lipid Res.* 62: 55–74.

Hou, Q., Ufer, G. and Bartels, D. (2016) Lipid signalling in plant responses to abiotic stress. *Plant Cell Environ.* 39: 1029–1048.

Katagiri, T., Takahashi, S. and Shinozaki, K. (2001) Involvement of a novel Arabidopsis phospholipase D, *AtPLDδ*, in dehydration-inducible accumulation of phosphatidic acid in stress signalling. *Plant J.* 26: 595–605.

Laxalt, A.M., Ter, R.B., Verdonk, J.C., Parigi, L., Wil, T. and Vossen, J. (2001) Characterization of five tomato phospholipase D cDNAs: rapid and specific expression of LePLDbeta1 on elicitation with xylanase. *Plant J.* 26: 237–247.

Lee, S. and Choi, D. (2013) Comparative transcriptome analysis of pepper (*Capsicum annuum*) revealed common regulons in multiple stress conditions and hormone treatments. *Plant Cell Rep.* 32, 1351–1359.

Lei, P., Xu, Z., Liang, J., Luo, X., Zhang, Y., Feng, X., et al. (2016) Poly(γ-glutamic acid) enhanced tolerance to salt stress by promoting proline accumulation in *Brassica napus*, L. *Plant Growth Regul.* 78: 1–9.

Li, W., Li, M., Zhang, W., Welti, R. and Wang, X. (2004) The plasma membrane-bound phospholipase Dδ enhances freezing tolerance in *Arabidopsis thaliana*. *Nature Biotechnol.* 22: 427–433.

Li, M., Hong, Y. and Wang, X. (2009) Phospholipase D- and phosphatidic acid-mediated signaling in plants. *Biochem. Biophys. Acta* 1791: 927–935.

Li, T., Xu, X., Li, Y., Wang, H., Li, Z. and Li, Z. (2015) Comparative transcriptome analysis reveals differential transcription in heat-susceptible and heat-tolerant pepper (*Capsicum annum*, L.) cultivars under heat stress. *J. Plant Biol.* 58: 411–424.

Lin, S., Yang, S., Li, X., Chen, F. and Zhang, M. (2016) Dynamics of water mobility and distribution in soybean antioxidant peptide powders monitored by lf-nmr. *Food Chem.* 199: 280–286.

Liu, L. (2013) Ultrastructural study on dynamics of lipid bodies and plastids during ripening of chili pepper fruits. *Micron* 46: 43–50.

Malacrida, C., Valle, E.M. and Boggio, S.B. (2006) Postharvest chilling induces oxidative stress response in the dwarf tomato cultivar Micro-Tom. *Physiol. Plant.* 127: 10–18.

Mao, L.C., Wang, G.Z., Zhu, C.G. and Pang, H.Q. (2007) Involvement of phospholipase D and lipoxygenase in response to chilling stress in postharvest cucumber fruits. *Plant Sci.* 172: 400–405.

Marigheto, N., Venturi, L. and Hills, B. (2008) Two-dimensional nmr relaxation studies of apple quality. *Postharvest Biol.Technol*. 48: 331–340.

Mateos, R.M., Jiménez, A., Román, P., Romojaro, F., Bacarizo, S., Leterrier, M., et al. (2013) Antioxidant systems from pepper (*Capsicum annuum*, L.): involvement in the response to temperature changes in ripe fruits. *Int. J. Mol. Sci.* 14: 9556–9580.

Meng, X. and Min, Z. (2012) Extending shelf-life of fresh-cut green peppers using pressurized argon treatment. *Postharvest Biol. Technol.* 71: 13–20.

Moellering, E.R., Muthan, B. and Benning, C. (2010) Freezing tolerance in plants requires lipid remodeling at the outer chloroplast membrane. *Science* 330: 226–228.

Munnik, T. and Laxalt, A.M. (2013) Measuring PLD activity in vivo. *Methods Mol. Biol.* 1009: 219–231.

Muzi, C., Camoni, L., Visconti, S. and Aducci, P. (2016) Cold stress affects H^+-ATPase and phospholipase D activity in Arabidopsis. *Plant Physiol. Biochnol.* 108: 328–336.

Nejadsadeghi, L., Maaliamiri, R., Zeinali, H., Ramezanpour, S. and Sadeghzade, B. (2015) Membrane fatty acid compositions and cold-induced responses in tetraploid and hexaploid wheats. *Mol. Biol. Rep.* 42: 363–372.

Pablo, T., Kirstin, F. and Ivo, F. (2015) An enhanced plant lipidomics method based on multiplexed liquid chromatography–mass spectrometry reveals additional insights into cold- and drought-induced membrane remodeling. *Plant J.* 84: 621–633.

Rajashekar, C.B., Zhou, H.E., Zhang, Y., Li, W. and Wang, X. (2006) Suppression of phospholipase Dalpha1 induces freezing tolerance in Arabidopsis: response of cold-responsive genes and osmolyte accumulation. *J. Plant Physiol.* 163: 916–926.

Rwm, F., Wang, C.Y., Smith, D.L., Gross, K.C. and Tian, M. (2004) MeSA and MeJA increase steady-state transcript levels of alternative oxidase and resistance against chilling injury in sweet peppers (*Capsicum annuum*, L.). *Plant Sci.* 166: 711–719.

Saita, E., Albanesi, D. and de Mendoza, D. (2016) Sensing membrane thickness: lessons learned from cold stress. *Biochim. Biophys. Acta* 1861: 837–846.

Shao, X. and Li, Y. (2013) Application of low-field NMR to analyze water characteristics and predict unfrozen water in blanched sweet corn. *Food Bioprocess Technol.* 6: 1593–1599.

Sharma, S. and Verslues, P.E. (2011) Essential role of tissue-specific proline synthesis and catabolism in growth and redox balance at low water potential. *Plant Physiol*. 157: 292–304.

Sinensky, M. (1974) Homeoviscous adaptation—a homeostatic process that regulates the viscosity of membrane lipids in *Escherichia coli*. *Proc. Natl. Acad. Sci. USA* 71: 522–525.

Snaar, J.E. and Van As, H. (1992) Probing water compartments and membrane permeability in plant cells by H NMR relaxation measurements. *Biophys J.* 63: 1654–1658.

Szymanski, J., Brotman, Y., Willmitzer, L. and Cuadrosinostroza, Á. (2014) Linking gene expression and membrane lipid composition of Arabidopsis. *Plant Cell* 26: 915–928.

Testerink, C. and Munnik, T. (2011) Molecular, cellular, and physiological responses to phosphatidic acid formation in plants. *J. Exp. Bot.* 62: 2349–2361.

Tiwari, K. and Paliyath, G. (2011) Cloning, expression and functional characterization of the C2 domain from tomato phospholipase Dα. *Plant Physiol. Biochtechnol.* 49: 18–32.

Torres-Franklin, M., Gigon, A., De Melo, D. and Zuily-Fodil, Y.T.A. (2007) Drought stress and rehydration affect the balance between MGDG and DGDG synthesis in cowpea leaves. *Physiol. Plant.* 131: 201–210.

Wang, Q., Ding, T., Gao, L., Pang, J. and Yang, N. (2012) Effect of brassinolide on chilling injury of green bell pepper in storage. *Sci. Hortic.* 144: 195–200.

Wang, Q., Ding, T., Zuo, J., Gao, L. and Fan, L. (2016) Amelioration of postharvest chilling injury in sweet pepper by glycine betaine. *Postharvest Biol. Technol.* 112: 114–120.

Welti, R., Li, W., Li, M., Sang, Y., Biesiada, H., Zhou, H.E., et al. (2002) Profiling membrane lipids in plant stress responses. *J. Biol. Chem.* 277: 31994–32002.

Wise, R.R. (1995) Chilling-enhanced photooxidation: the production, action and study of reactive oxygen species produced during chilling in the light. *Photosynth. Res.* 45: 79–97.

Xiao, S., Gao, W., Chen, Q.F., Chan, S.W., Zheng, S.X., Ma, J., et al. (2010) Overexpression of Arabidopsis Acyl-CoA binding protein ACBP3 promotes starvation-induced and age-dependent leaf senescence. *Plant Cell* 22: 1463–1482.

Xu, W.T., Peng, X.L., Luo, Y.B., Wang, J.A., Xing, G. and Huang, K.L. (2009) Physiological and biochemical responses of grapefruit seed extract dip on 'Redglobe' grape. *LWT - Food Sci. Technol.* 42: 471–476.

Yamada, T., Kuroda, K., Jitsuyama, Y., Takezawa, D., Arakawa, K. and Fujikawa, S. (2002) Roles of the plasma membrane and the cell wall in the responses of plant cells to freezing. *Planta* 215: 770–778.

Zhao, M.G., Chen, L., Zhang. L.L. and Zhang, W.H. (2009) Nitric reductase dependent nitric oxide production is involved in cold acclimation and freezing tolerance in Arabidopsis. *Plant Physiol.* 151: 755–767.

Zeng, F., Jiang, T., Wang, Y. and Luo, Z. (2015) Effect of UV-C treatment on modulating antioxidative system and proline metabolism of bamboo shoots subjected to chilling stress. *Acta Physiol. Plant.* 37: 1–10.